Epidemic dynamics on temporal complex networks

Ziting Luo,[1,2] Chengzuo Zhuge,[1,2] and Wei Chen[3,*]
[1]*School of Mathematical Sciences, Beihang University, Beijing 100191, China*
[2]*Key Laboratory of Mathematics, Informatics and Behavioral Semantics (LMIB), Beihang University, Beijing 100191, China*
[3]*School of Systems Science, Beijing Normal University, Beijing 100875, China*

(Received 28 January 2026; accepted 17 July 2026; published 11 August 2026)

A wide range of real-world systems, ranging from physical and biological systems to social systems, can be described as temporal networks, where link temporality has profound effects on many dynamical processes taking place on networks. Here we study the susceptible-infected-susceptible model on temporal complex networks, where edges are randomly activated or terminated at each time step. We analytically obtain the epidemic threshold for temporal complex networks with arbitrary initial degree distributions. The approximate endemic equilibrium prevalence for temporal complex networks with arbitrary initial degree distributions is derived analytically for the system close to the epidemic threshold and far away from it. In addition, we demonstrate that the system undergoes a continuous transition from the disease-free state to the endemic state. Our results pave the way to understand how the degree distributions will affect a wide variety of binary-state dynamics on temporal complex networks.

DOI: 10.1103/48z3-6cmb

I. INTRODUCTION

In the last decade, dynamical processes on networks have been extensively studied with many applications in social, technological, and biological systems [1–6]. Traditional studies about this topic mainly focused on static networks [7–10], whose links offer permanent connections between nodes. Yet, it is increasingly recognized that many social and natural systems are characterized by temporal networks where link temporality affects the dynamical processes that take place on networks, from information diffusion [11–14] to epidemic spreading [15–17], cooperation [18–20], and synchronization [21–25]. For example, social contact networks underlying the epidemic processes are mostly temporal networks, where the link temporality can notably slow down or promote the disease outbreak [26]. The functional brain networks, characterizing the interactions among different regions of the brain, can also evolve over time, where the link temporality can affect its temporal stability [27].

The effect of link temporality on the dynamical processes on networks has been a subject of high interest in many disciplines [28–36]. A number of analytically tractable modeling paradigms have been proposed to characterize the link temporality of networks. The edge-Markovian dynamic network is an analytically tractable framework for temporal networks that has been widely studied and used [37–39]. Volz and Meyers investigated how social mixing affects disease spreading within the susceptible-infected-recovered (SIR) framework [40,41]. They proposed the neighbor-exchange mechanism, in which two edges are sampled uniformly at random and their endpoints are swapped, thereby altering the network topology while preserving node degrees. However, during the evolution of many real-world social networks, the degree of each node is not always preserved. Subsequent representative studies, notably the edge activation-termination model, relaxed the fixed-degree assumption by allowing each node to randomly break existing links and form new links at constant rates [42–45]. Related models incorporated edge activation and deactivation with fixed underlying network topology, allowing each node to temporarily deactivate its links to infectious neighbors and reactivate them once those neighbors are not infectious [46,47]. In addition, considering that the network topology may adaptively change with time depending on the dynamical state of nodes, many adaptive network models have been proposed to study the dynamical processes on networks [48–50]. Despite these developments, previous studies only focus on the epidemic processes on temporal networks with initial Poisson degree distribution. Many real-world temporal networks have heterogeneous degree distributions, such as scale-free degree distributions [51]. While the effects of heterogeneity on epidemic dynamics on temporal networks have already been investigated in some paradigms, such as activity-driven networks [33,52,53] and temporal-switching networks [32,54,55], it is still an open question how the degree distributions will affect the epidemic dynamics on edge-Markovian dynamics networks.

In this paper, we address the above problem by considering a prototypical dynamical process, the susceptible-infected-susceptible (SIS) process, on temporal complex networks with arbitrary degree distributions, where edges are randomly activated or terminated. We apply a tractable pair-approximation approach to analytically derive the epidemic threshold. With the asymptotic method, analytical approximations for the endemic equilibrium prevalence are derived for the system close to the epidemic threshold and far away from it. Compared with the traditional closure model, our framework shows better agreement with Monte Carlo simulations. In addition, we

*Contact author: chwei@bnu.edu.cn

demonstrate that the system undergoes a continuous transition from the disease-free state to the endemic state.

This paper is organized as follows. In Sec. II, we study the SIS model on a temporal complex network with edge activation and termination. In Sec. III, we derive the degree moments at the steady state. We derive the epidemic threshold of the system and demonstrate that a forward transcritical bifurcation occurs at this critical point. In Sec. IV, we derive the analytical approximation for the endemic equilibrium states. We analyze the effects of the transmission rate, the edge activation rate, and the edge termination rate on epidemic dynamics. Finally, our results will be discussed and concluded in Sec. V.

II. MODEL

We consider a susceptible-infected-susceptible (SIS) model in a network consisting of N nodes. The state of the nodes in the network can be either infected or susceptible. Infected nodes can infect their susceptible neighbors at a rate τ, while infected nodes recover from the disease at a rate γ, becoming susceptible again. The network evolves by randomly adding edges at a rate α and deleting edges at a rate ω. This leads to a system of five coupled ordinary differential equations,

$$\begin{aligned}
[\dot{S}] &= \gamma[I] - \tau[SI],\\
[\dot{I}] &= \tau[SI] - \gamma[I],\\
[\dot{SS}] &= 2\gamma[SI] - 2\tau[SSI] + \alpha([S]([S]-1) - [SS]) - \omega[SS],\\
[\dot{SI}] &= -(\tau+\gamma)[SI] + \tau([SSI] - [ISI]) + \gamma[II]\\
&\quad + \alpha([S][I] - [SI]) - \omega[SI],\\
[\dot{II}] &= -2\gamma[II] + 2\tau([ISI] + [SI]) + \alpha[I]([I]-1)\\
&\quad - \alpha[II] - \omega[II],
\end{aligned} \tag{1}$$

where $[S]$ is the expected number of susceptible nodes and $[I]$ is the expected number of infected nodes. $[AB]$ represents the expected number of edges connecting a node in state A to a node in state B. $[ABC]$ denotes the expected number of triples, $A-B-C$, of an individual in state A connected to an individual in state B connected to an individual in state C. Specifically, $[ABC] = \sum_{i,j,k} a_{ij}a_{jk}A_iB_jC_k$, where $G = (a_{ij})_{N\times N}$ is the adjacency matrix of the network. The middle node B is the central node of the triple. A, B, C can be either the state S or I [56,57]. The first two equations describe susceptible nodes being infected by infected neighbors through SI edges at a rate τ, and infected nodes recovering to susceptible nodes at a rate γ. In the third equation, the first term represents SI edges in which the infected node recovers, converting SI edges to SS edges; the second term represents the decrease of SS edges due to susceptible nodes in SSI triples being infected; the third term represents the addition of new SS edges among all pairs of susceptible nodes at a rate α; and the fourth term represents the deletion of existing SS edges at a rate ω. The dynamics of SI and II edges can be interpreted in the same way.

Since Eqs. (1) depend on higher-order moments, a closure approximation is required to obtain a self-consistent solvable system. To make our model analytically tractable, we apply a pair-approximation approach, the supercompact pairwise model [58], to simplify Eqs. (1). This approach leads to the following formula for the expected number of triples:

$$[ASI] \approx [AS][SI]\left(\frac{[S]}{([SS]+[SI])^2}\tilde{A} + \frac{1}{[SS]+[SI]}\tilde{B}\right), \tag{2}$$

where $\tilde{A} = \frac{\langle k^2\rangle^2 - \langle k\rangle\langle k^3\rangle}{\langle k^2\rangle - \langle k\rangle^2}$ and $\tilde{B} = \frac{\langle k^3\rangle - \langle k^2\rangle\langle k\rangle}{\langle k^2\rangle - \langle k\rangle^2} - 1$, k is the degree of a node, $\langle k\rangle$ is the average degree, and $\langle k^2\rangle$, $\langle k^3\rangle$ are the second and third moments of the degree distribution, respectively.

To ensure that the triplet approximation accurately captures the network dynamics, it is important to describe how the degree distribution and its moments evolve over time. For any node with degree k, its k edges may be deleted at a rate ω, while the remaining $N-1-k$ potential edges may be added at a rate α. The evolution of the degree of the node thus forms a continuous-time Markov chain. Therefore, we use the Kolmogorov equation to describe the temporal evolution of the degree distribution, which is $\dot{p}_k = \alpha(N-k)p_{k-1} - [\alpha(N-1-k) + \omega k]p_k + \omega(k+1)p_{k+1}$. The first term of the equation describes the transition of a node with degree $k-1$ to degree k via the addition of a new edge, as a node with degree $k-1$ has $N-k$ potential nonexisting edges, each of which can be added at a rate α. The second term represents the loss term, accounting for nodes of degree k leaving the current state through two processes: addition of a new edge at a rate $\alpha(N-1-k)$ (transition to degree $k+1$) or deletion of an existing edge at a rate ωk (transition to degree $k-1$). The third term describes the transition of nodes with degree $k+1$ to degree k due to the deletion of an existing edge at a rate ω. To systematically characterize the evolution of the first three moments of the degree distribution, we apply a generating function approach, where the generating function for the degree distribution is defined as $g(x,t) = \sum_{k=0}^{N-1} p_k(t)x^k$. Through direct algebraic manipulation, we derive the following partial differential equation satisfied by the generating function of the degree distribution: $\frac{\partial g}{\partial t} = (x-1)(\alpha(N-1)g - (\alpha x + \omega)\frac{\partial g}{\partial x})$. Since $\langle k\rangle = g_x(1,t)$, $\langle k^2\rangle = g_{xx}(1,t) + g_x(1,t)$, and $\langle k^3\rangle = g_{xxx}(1,t) + 3g_{xx}(1,t) + g_x(1,t)$, we obtain the dynamical equations for the first three moments of the degree distribution as

$$\begin{aligned}
\dot{\langle k\rangle} &= \alpha(N-1) - (\alpha+\omega)\langle k\rangle,\\
\dot{\langle k^2\rangle} &= \alpha(N-1) + (2N\alpha - 3\alpha + \omega)\langle k\rangle - 2(\alpha+\omega)\langle k^2\rangle,\\
\dot{\langle k^3\rangle} &= \alpha(N-1) + (3N\alpha - 4\alpha - \omega)\langle k\rangle\\
&\quad + (3N\alpha - 6\alpha + 3\omega)\langle k^2\rangle - 3(\alpha+\omega)\langle k^3\rangle.
\end{aligned} \tag{3}$$

Equations (1)–(3) are the mathematical framework of our model, which describes the epidemic process on heterogeneous networks with random edge activation and termination.

To validate the effectiveness of our model, we consider the traditional closure model based on the widely used triplet approximation, $[ASI] = [(\langle k\rangle - 1)/\langle k\rangle][AS][SI]/[S]$ [59]. We compare the analytical results of our model and the traditional closure model with the results obtained from Monte Carlo simulations for Erdös-Rényi networks with random link addition and deletion dynamics and Barabási-Albert networks with random link addition and deletion dynamics as shown in Fig. 1. As shown in Fig. 1(a), on the Erdős-Rényi network with random link addition and deletion dynamics,

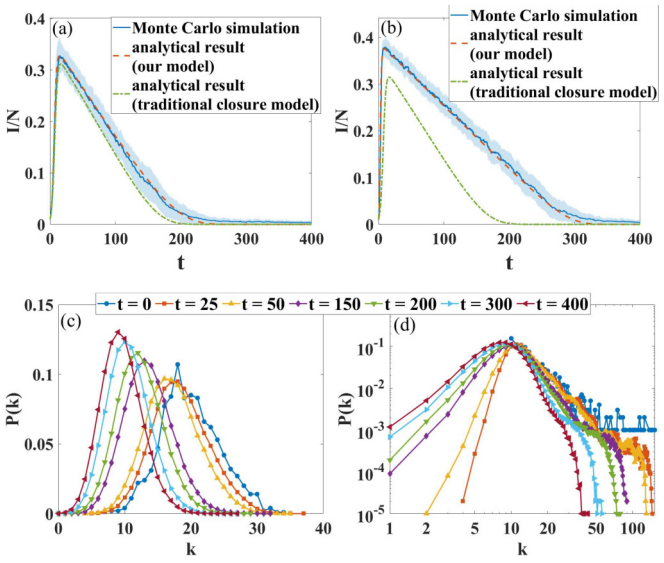

FIG. 1. Evolution of infection density and degree distribution. (a) and (b) Time evolution of the infection density I/N on (a) an Erdős-Rényi network and (b) a Barabási-Albert network. The Monte Carlo simulations are averaged over 100 independent realizations. (c) and (d) The degree distribution $P(k)$ at various time steps t for (c) the Erdős-Rényi network on a linear scale and (d) the Barabási-Albert network on a log-log scale. Parameter settings for all panels are $N = 1000$, $\tau = 0.08$, $\gamma = 1$, $\alpha = 0.00004$, and $\omega = 0.005$.

the results of both analytical methods are consistent with the Monte Carlo simulations within the error range. The degree distribution of the network remains approximately Poisson-like throughout the evolution and gradually converges to the stationary state in Fig. 1(c). However, in Fig. 1(b), on the Barabási-Albert network with the random link addition and deletion dynamics, the results of the traditional closure model show a significant deviation from the Monte Carlo simulation results, while the results of our model remain highly consistent with the Monte Carlo simulation results. This is because the initial degree distribution of the Barabási-Albert network is heterogeneous. During the early and intermediate transient stages, the degree distribution is heterogeneous. High-degree nodes have a significant influence on the spreading dynamics in Fig. 1(d). Since our model explicitly considers degree heterogeneity, it can more accurately capture this transient evolution process. To quantitatively compare the predictive performance of different methods, we use the normalized Euclidean distance (NED) to measure the error between the analytical results obtained from our model, those from the traditional closure model, and the Monte Carlo simulation, which is defined as

$$\mathrm{NED} = \frac{\sqrt{\sum_{t=t_0}^{T}[I(t)-\hat{I}(t)]^2}}{\sqrt{\sum_{t=t_0}^{T}[I^2(t)+\hat{I}^2(t)]}}. \tag{4}$$

In Fig. 1(a), the error between the analytical results of our model and the Monte Carlo simulation results for the epidemic prevalence is 2.935%, whereas the error between the analytical results of the traditional closure model and the Monte Carlo simulation results is 11.50%. In Fig. 1(b), the error between the analytical results of our model and the Monte Carlo simulation results is 2.336%, whereas the error between the analytical results of the traditional closure model and the Monte Carlo simulation results is 40.83%. Furthermore, as Fig. 2 shows, the analytical predictions of the first three moments are in excellent agreement with Monte Carlo simulations on Barabási-Albert networks with random link addition and deletion dynamics.

III. THE DERIVATION OF THE EPIDEMIC THRESHOLD

For temporal networks with homogeneous degree distributions, a closed-form expression for the epidemic threshold, above which the total number of infected individuals reaches a finite fraction of the network, has been reported in prior work [60]. We next calculate the epidemic threshold for temporal networks with heterogeneous degree distributions by measuring the largest real part of the eigenvalues of the Jacobian matrix which can be used to determine whether the disease-free equilibrium is stable. Specifically, the largest real part of the eigenvalues of the Jacabian matrix is negative once the disease-free equilibrium is stable, while it is positive once the disease-free equilibrium is unstable. Therefore, the epidemic threshold can be identified by determining whether the largest real part of the eigenvalues of the Jacobian matrix is zero. To analytically obtain the epidemic threshold, we first reduce the dimensionality of the system by applying the conservation equations for the nodes and the edges, i.e., $[S]+[I]=N$ and $[SS]+2[SI]+[II]=\langle k\rangle N$, respectively. This leads to the following simplified form of Eqs. (1):

$$\begin{aligned}
[\dot{I}] &= \tau[SI]-\gamma[I],\\
[\dot{SI}] &= -(\tau+\gamma)[SI]+\gamma[II]+\tau[SI](\langle k\rangle N-[II]-3[SI])\\
&\quad\times\left(\frac{(N-[I])\tilde{A}}{(\langle k\rangle N-[II]-[SI])^2}+\frac{\tilde{B}}{\langle k\rangle N-[II]-[SI]}\right)\\
&\quad+\alpha[(N-[I])[I]-[SI]]-\omega[SI],\\
[\dot{II}] &= -2\gamma[II]+2\tau[SI]+2\tau[SI]^2\left(\frac{(N-[I])\tilde{A}}{(\langle k\rangle N-[II]-[SI])^2}\right.\\
&\quad\left.+\frac{\tilde{B}}{\langle k\rangle-[II]-[SI]}\right)+\alpha[[I]([I]-1)]-(\alpha+\omega)[II].
\end{aligned} \tag{5}$$

Then we evaluate the Jacobian matrix of the system at the disease-free equilibrium based on Eqs. (3) and (5). Specifically, once the system reaches the disease-free equilibrium, the degree distribution becomes stationary and the first three moments of the degree distribution satisfy $\langle\dot{k}\rangle=\langle\dot{k^2}\rangle=\langle\dot{k^3}\rangle=0$. By applying Eq. (3), we have

$$\begin{aligned}
\langle k\rangle_{\mathrm{eq}} &= \frac{\alpha(N-1)}{\alpha+\omega},\\
\langle k^2\rangle_{\mathrm{eq}} &= \frac{\alpha^2(N-1)^2+\alpha\omega(N-1)}{(\alpha+\omega)^2},\\
\langle k^3\rangle_{\mathrm{eq}} &= \frac{\alpha^3(N-1)^3+3\omega(N-1)^2\alpha^2}{(\alpha+\omega)^3}\\
&\quad+\frac{\alpha\omega(N-1)(-\alpha+\omega)}{(\alpha+\omega)^3},
\end{aligned} \tag{6}$$

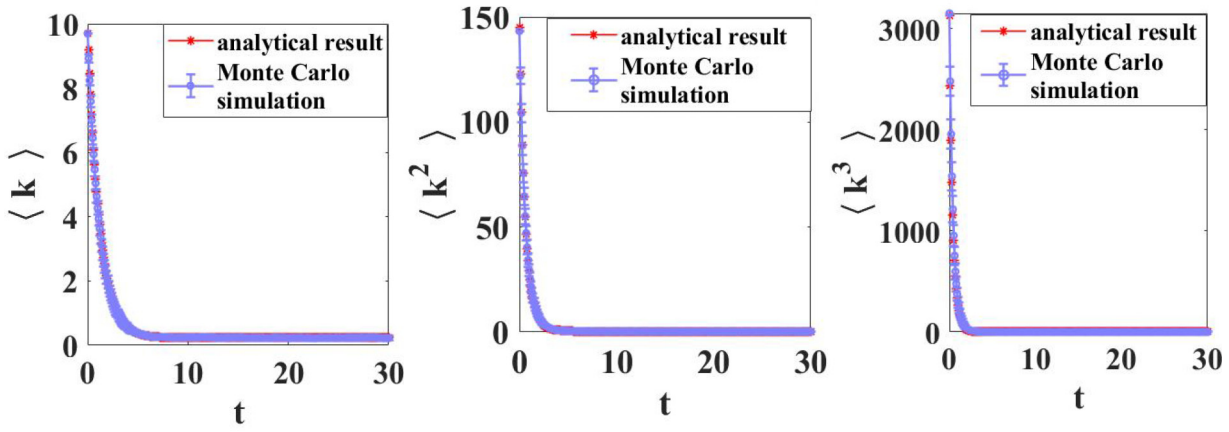

FIG. 2. The evolution of the first, second, and third moments of the degree distribution with time, namely, $\langle k\rangle$, $\langle k^2\rangle$, and $\langle k^3\rangle$, respectively, in (a)–(c) on Barabási-Albert networks with random link addition and deletion dynamics, with $N = 100$, $\tau = 0.5$, $\gamma = 0.05$, $\alpha = 0.002$ and $\omega = 0.85$. Red dots represent the analytical results of our model and the blue solid lines represent the results from Monte Carlo simulations.

where $\langle k\rangle_{\rm eq}$, $\langle k^2\rangle_{\rm eq}$, and $\langle k^3\rangle_{\rm eq}$ are the first three steady-state moments of the degree distribution. Here we denote them by k_1, k_2, and k_3, respectively. Moreover, since all individuals are susceptible at the disease-free equilibrium, we have $([I], [SI], [II]) = (0, 0, 0)$. We thus obtain the Jacobian matrix at the disease-free (DF) equilibrium as

$$\mathrm{DF} = \begin{bmatrix} J_1 & 0 \\ 0 & J_2 \end{bmatrix}, \tag{7}$$

where

$$J_1 = \begin{bmatrix} -\gamma & \tau & 0 \\ N\alpha & -\alpha-\gamma-\omega+\tau\left(-2+\frac{k_2}{k_1}\right) & \gamma \\ -\alpha & 2\tau & -\alpha-2\gamma-\omega \end{bmatrix}$$

and

$$J_2 = \begin{bmatrix} -\alpha-\omega & 0 & 0 \\ 2N\alpha-3\alpha+\omega & -2\alpha-2\omega & 0 \\ 3N\alpha-4\alpha-\omega & 3N\alpha-6\alpha+3\omega & -3\alpha-3\omega \end{bmatrix}.$$

Since J_2 is a lower triangular matrix, its eigenvalues are given by its diagonal entries, all of which are negative. Therefore, the stability of the disease-free equilibrium depends on the eigenvalues of J_1, whose characteristic polynomial is given by $\lambda^3 + a_1\lambda^2 + a_2\lambda + a_3$ with $a_1 = 2\alpha + 4\gamma + 2\omega - \tau(\frac{k_2}{k_1} - 2)$, $a_2 = \alpha^2 + 5\alpha\gamma + 2\omega\alpha + 5\gamma^2 + 5\gamma\omega + \omega^2 - \tau(N\alpha - 2\alpha + \frac{k_2}{k_1}\alpha - 4\gamma + 3\gamma\frac{k_2}{k_1} - 2\omega + \frac{k_2}{k_1}\omega)$, and $a_3 = \alpha^2\gamma + 3\alpha\gamma^2 + 2\alpha\gamma\omega + 2\gamma^3 + 3\gamma^2\omega + \gamma\omega^2 - \tau(N\alpha^2 + 2N\alpha\gamma + N\alpha\omega - 3\alpha\gamma + \gamma\alpha\frac{k_2}{k_1} - 2\gamma^2 + 2\gamma^2\frac{k_2}{k_1} - 2\gamma\omega + \gamma\omega\frac{k_2}{k_1})$.

To determine the stability of the disease-free equilibrium, we apply the Routh-Hurwitz criterion [61]. According to this criterion, all roots of the characteristic polynomial have a negative real part, i.e., the steady state of the disease-free equilibrium is asymptotically stable, once $a_1 > 0$, $a_1a_2 > a_3$, and $a_3 > 0$ simultaneously hold. As demonstrated in Appendix A, the condition $a_3 > 0$ is sufficient to imply $a_1 > 0$ and $a_1a_2 > a_3$. Therefore, the stability of the disease-free equilibrium is fully determined by the sign of a_3, which equals $-\mathrm{Det}(J_1)$. By solving the equation $\mathrm{Det}(J_1) = 0$ with respect to the transmission rate τ, we obtain the epidemic threshold,

$$\tau_c = \frac{(\alpha+\gamma+\omega)\gamma(\alpha+2\gamma+\omega)}{(\alpha+\gamma+\omega)[N\alpha+2\gamma(k_2/k_1-1)]-\gamma\omega}. \tag{8}$$

Specifically for homogeneous networks with the average degree $\langle k\rangle$, we simplify the triplet approximation equation (2) to the traditional closure, $[ASI] = [(\langle k\rangle - 1)/\langle k\rangle][AS][SI]/[S]$. Under this simplified form, we obtain the epidemic threshold,

$$\bar{\tau}_c = \frac{\gamma(\alpha+2\gamma+\omega)}{N\alpha+2\gamma(k_1-1)}. \tag{9}$$

Figure 3(a) shows the critical surface of the epidemic threshold as a function of the edge activation rate and the edge termination rate by performing simulation with Eq. (8). Specifically, as Fig. 3(b) shows, for low edge activation rate, the epidemic threshold decreases rapidly as the edge activation rate increases, and asymptotically approaches zero. On the other hand, as Fig. 3(c) shows, the epidemic threshold increases rapidly with the edge termination rate for low edge activation rate, while it increases very slowly with the edge termination rate once the edge activation rate is sufficiently high.

The investigation into the continuity of phase transitions in epidemic dynamics is critical for predicting the likelihood of large-scale spreading events, providing a scientific foundation for the development of effective prevention and control strategies [32]. Here we apply the left and right eigenvectors associated with the zero eigenvalue of the Jacobian matrix at the disease-free equilibrium to determine whether the bifurcation is forward (i.e., the transition is continuous), based on a theorem proposed by Castillo-Chavez and Song [62]. Specifically, by reducing Eq. (1) with the conservation equations for

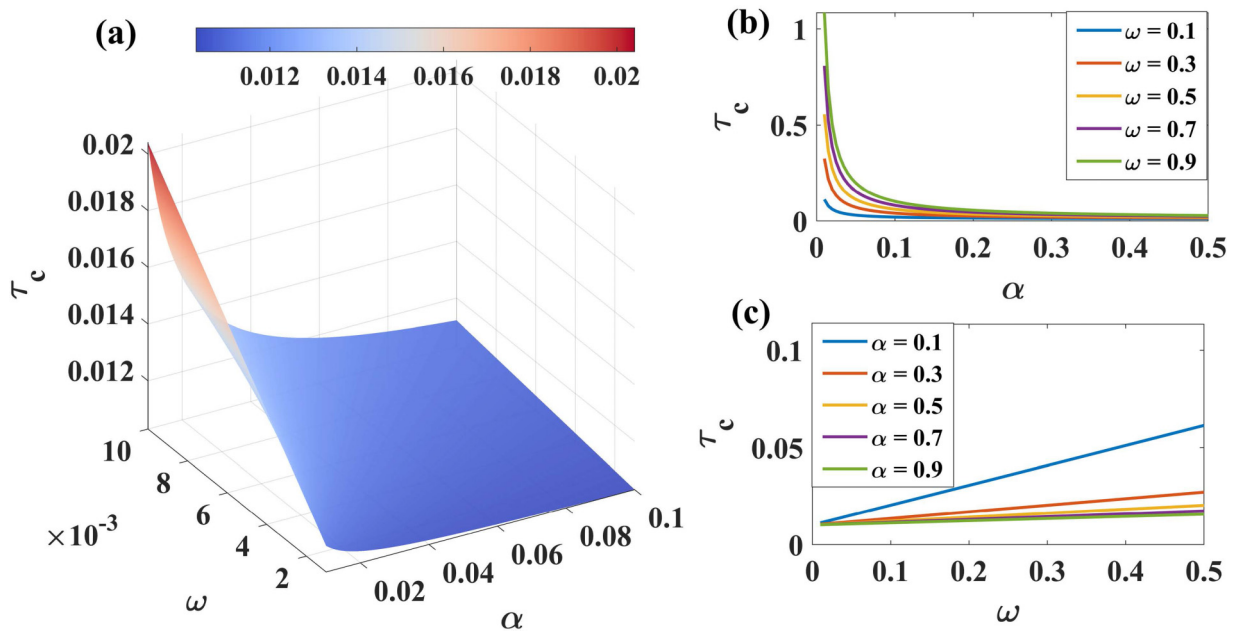

FIG. 3. (a) Critical surface (τ_c, α, ω) defined by Eq. (8), with $\gamma = 1$ and $N = 100$. The epidemic threshold τ_c vs α in (b) and ω in (c).

the nodes and the edges, we obtain

$$
\begin{aligned}
[\dot{I}] &= \tau[SI] - \gamma[I], \\
[\dot{SS}] &= 2\gamma[SI] - 2\tau[SS]\left(\frac{(N-[I])\tilde{A}[SI]}{([SS]+[SI])^2} + \frac{\tilde{B}[SI]}{[SS]+[SI]}\right) \\
&\quad + \alpha(N-[I])(N-[I]-1) - (\alpha+\omega)[SS], \\
[\dot{SI}] &= -(\tau+\gamma)[SI] + \gamma\big(\langle k\rangle N - [SS] - 2[SI]\big) \\
&\quad + \tau([SS]-[SI])\left(\frac{(N-[I])\tilde{A}[SI]}{([SS]+[SI])^2} + \frac{\tilde{B}[SI]}{[SS]+[SI]}\right) \\
&\quad + \alpha(N-[I])[I] - (\alpha+\omega)[SI]. \qquad (10)
\end{aligned}
$$

By performing a linear analysis around the disease-free equilibrium, $(0, 0, k_1N)$, and ignoring the higher-order terms, we obtain the Jacobian matrix of the system with $\tau = \tau_c$,

$$
J(0,0,k_1N) = \begin{bmatrix} -\gamma & \tau & 0 \\ N\alpha & -\alpha - 3\gamma - \omega + \tau_c(-2 + k_2/k_1) & -\gamma \\ \alpha(1-2N) & 2\gamma - 2\tau_c\left(-1 + \frac{k_2}{k_1}\right) & -\alpha - \omega \end{bmatrix}. \qquad (11)
$$

Then we obtain the right non-negative eigenvector $m = [R_0 \quad R_1 \quad R_2]^\top$ and the left eigenvector $u = [(N\alpha^2 + 2N\alpha\gamma + N\alpha\omega - \alpha\gamma)/(\gamma^2) \quad (\alpha+\omega)/\gamma \quad -1]^\top$ corresponding to the zero eigenvalue of $J(0,0,k_1N)$, where $R_0 = \alpha^2k_1 + 3\alpha\gamma k_1 + 2\alpha k_1\omega + 2\gamma^2k_1 + 3\gamma k_1\omega + k_1\omega^2$, $R_1 = N\alpha^2k_1 + 2N\alpha\gamma k_1 + N\alpha k_1\omega - 3\alpha\gamma k_1 + \alpha\gamma k_2 - 2\gamma^2k_1 + 2\gamma^2k_2 - 2\gamma k_1\omega + \gamma k_2\omega$, and $R_2 = -2N\alpha^2k_1 - 4N\alpha\gamma k_1 - 2N\alpha k_1\omega + \alpha^2k_1 + 5\alpha\gamma k_1 - 2\alpha\gamma k_2 + \alpha k_1\omega + 2\gamma^2k_1 - 4\gamma^2k_2 + 2\gamma k_1\omega - 2\gamma k_2\omega$. Thus we have $\sum_{k,i,j=1}^{3} u_k m_i m_j \frac{\partial^2 F_k}{\partial X_i \partial X_j}(\mathbf{X}^*, 0) < 0$ and $\sum_{k,i=1}^{3} u_k m_i \frac{\partial^2 F_k}{\partial X_i \partial \phi}(\mathbf{X}^*, 0) > 0$, where $X_1 = [I]$, $X_2 = [SI]$, $X_3 = [SS]$, $\mathbf{X}^* = (0, 0, k_1N)$, $\phi = \tau - \tau_c$, and $F_k(\mathbf{X}, \phi) = [\dot{X}_k]$, $k = 1, 2, 3$. This indicates that the phase transition is continuous based on the theorem proposed by Castillo-Chavez and Song. The detailed derivation of this result can be found in Appendix B.

IV. THE ENDEMIC EQUILIBRIUM STATES

Due to the high dimensionality and pronounced nonlinearity of Eqs. (1), previous studies have found it intractable to obtain an exact analytical expression of the endemic equilibrium. Here, based on the regular perturbation method [63], we derive the approximations of the endemic equilibrium on temporal networks with arbitrary degree distributions. In order to turn the task of deriving the endemic equilibrium from Eq. (1) into a perturbation problem, we first nondimensionalize the system to reduce the number of independent parameters by defining $v = [S]/N$, $w = [I]/N$, $x = [SI]/k_1N$, $y = [SS]/k_1N$, $z = [II]/k_1N$, and $T = t/\gamma$, $\tilde{\alpha} = \alpha/\gamma$, $\tilde{\omega} = \omega/\gamma$, $\delta = \tau/\gamma$, $\delta_c = \tau_c/\gamma$, when the system reaches the endemic equilibrium. By utilizing the equilibrium conditions $\dot{v} = \dot{x} = \dot{y} = 0$ at the endemic equilibrium, we reduce Eqs. (1) to the following polynomial equations:

$$
\begin{aligned}
M(x,y) &= \left(\frac{\delta_c}{\delta}\right)^2\left[(1-2x-y) - (\tilde{\alpha}+\tilde{\omega})\left(x + \frac{1}{2}y\right) + \left(\frac{\tilde{\alpha}N}{2k_1} - \frac{\tilde{\alpha}}{2k_1}\right)\right](x+y)^2 + \frac{\delta_c}{\delta}\left[-\delta_c x(x+y)^2 \right. \\
&\quad \left. - \lambda x^2 - \mu x^2(x+y) + \frac{\tilde{\alpha}}{2k_1}\sigma x(x+y)^2\right] \\
&\quad + \lambda\sigma x^3 - \frac{N\tilde{\alpha}}{2k_1}\sigma^2x^2(x+y)^2 = 0, \qquad (12)
\end{aligned}
$$

$$N(x,y)=\left(\frac{\delta_c}{\delta}\right)^2\left[2x-(\tilde{\alpha}+\tilde{\omega})y+\frac{\tilde{\alpha}N}{k_1}-\frac{\tilde{\alpha}}{k_1}\right](x+y)^2 + \frac{\delta_c}{\delta}\left[-2\lambda xy-2\mu xy(x+y)-2\frac{\tilde{\alpha}N}{k_1}\sigma x(x+y)^2 + \frac{\tilde{\alpha}}{k_1}\sigma x(x+y)^2\right]+2\lambda\sigma x^2y+\frac{N\tilde{\alpha}}{k_1}\sigma^2x^2(x+y)^2 = 0, \tag{13}$$

where $\sigma = k_1\delta_c$, $\lambda = [(k_2^2 - k_1k_3)/(k_2 - k_1^2)]\delta_c/k_1$, and $\mu = [(k_3 - k_1k_2)/(k_2 - k_1^2) - 1]\delta_c$. Note that we replace δ with $\delta_c \cdot \frac{\delta}{\delta_c}$ to find the small parameter in the system of polynomial equations (12) and (13).

To convert solving the polynomial equations (12) and (13) into a perturbation problem in the case that the system is close to the epidemic threshold, i.e., $\delta \approx \delta_c$ or $\tau \approx \tau_c$, we introduce the dimensionless small parameter $\eta = 1 - \frac{\delta_c}{\delta}$ and replace $\frac{\delta_c}{\delta}$ in Eqs. (12) and (13) with $1 - \eta$. Once the system is close to the epidemic threshold, the endemic equilibrium can be regarded as a small perturbation to the disease-free steady state, $(x, y) = (0, 1)$. By applying the implicit function theorem to linearize Eq. (12) around the point $(x, y) = (0, 1)$, we obtain

$$y = 1 - \left(2 + \frac{1}{1-\eta}C\right)x, \tag{14}$$

where $C = \frac{(2-\tilde{\alpha})\delta_c}{\tilde{\alpha}+\tilde{\omega}+2}$. By applying Eq. (14) and the asymptotic expansions for the variables x, y, and $\frac{1}{1-\eta}$ in terms of η around x_0, y_0, and 0, respectively, the left-hand side of Eq. (13) becomes a polynomial in η. Since the right-hand side of Eq. (13) is zero, we have that the coefficients at each order of η are zero. Thus, we obtain the approximate endemic equilibrium as

$$w_1^* = \frac{2k_1^2\gamma\tau_c(\alpha+\gamma+\omega)(\alpha+2\gamma+\omega)}{k_1\tau_c\left[N\alpha k_1\tau_c\left(k_2-k_1^2\right)+2\gamma\tau_c\left(k_2^2-k_1k_3\right)\right.} \eta + \left.2\gamma^2\left(k_3-k_2k_1-k_2+k_1^2\right)\right](\alpha+2\gamma+\omega) - 2\tau_c^2\gamma(2\gamma-\alpha)\left(k_2^2-k_1k_3\right),$$
$$x_1^* = \frac{2k_1\gamma^2(\alpha+\gamma+\omega)(\alpha+2\gamma+\omega)\left(k_2-k_1^2\right)}{k_1\tau_c\left[N\alpha k_1\tau_c\left(k_2-k_1^2\right)+2\gamma\tau_c\left(k_2^2-k_1k_3\right)\right.} \eta + \left.2\gamma^2\left(k_3-k_2k_1-k_2+k_1^2\right)\right](\alpha+2\gamma+\omega) - 2\tau_c^2\gamma(2\gamma-\alpha)\left(k_2^2-k_1k_3\right). \tag{15}$$

In the case that the system is far away from the epidemic threshold, i.e., $\delta \gg \delta_c$ or $\tau \gg \tau_c$, we choose $\varepsilon = \frac{\delta_c}{\delta}$ as the small nondimensional parameter. Since the transmission rate is significantly higher than the recovery rate for $\delta \gg \delta_c$, the disease is expected to spread throughout almost the entire network, leaving very few $[SS]$ edges, which implies $y \approx 0$. In this case, the endemic equilibrium can be regarded as a perturbation to the steady state, $y = 0$. Following the approach outlined in the case of $\delta \approx \delta_c$, we obtain the approximate endemic equilibrium as

$$w_2^* = 1 - \frac{\left(k_1^3+k_3-2k_1k_2\right)\gamma}{\left(k_1k_3-k_2^2\right)\tau_c}\varepsilon,$$
$$x_2^* = \frac{\gamma}{k_1\tau_c}\varepsilon - \frac{\left(k_1^3+k_3-2k_1k_2\right)\gamma^2}{\left(k_1k_3-k_2^2\right)k_1\tau_c^2}\varepsilon^2. \tag{16}$$

The full mathematical derivations are systematically presented in Appendix C for both cases when the system is close to the epidemic threshold and far away from it. To validate the accuracy of our approximation, we perform numerical integration of Eqs. (1) and compare the analytical results of the epidemic prevalence at steady state I^*/N across varying values of τ with approximate results w_1^* and w_2^* obtained from our approach. We test our approach on two types of heterogeneous networks: a bimodal network composed of nodes with degree three and five, and a Barabási-Albert network with average degree $\langle k\rangle = 19.8$. As Figs. 4(a) and 4(c) show, the approximate results agree well with the analytical results when the system is close to the epidemic threshold in both networks. Once the system is far away from the epidemic threshold, as shown in Figs. 4(b) and 4(d), the approximation closely matches with the analytical results, indicating the effectiveness of our approach in capturing epidemic dynamical

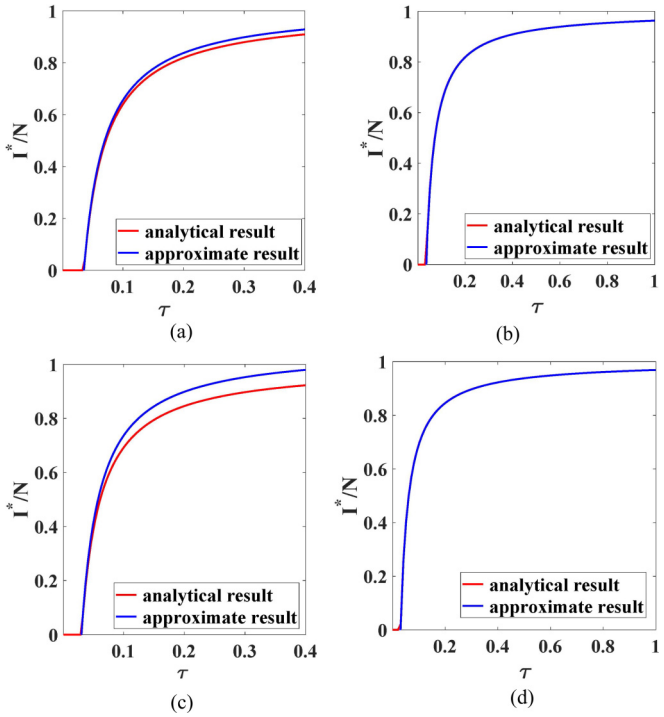

FIG. 4. Epidemic prevalence vs τ in the regime of $\tau \approx \tau_c$ in (a) and (c), but in the regime of $\tau \gg \tau_c$ in (b) and (d). The results in (a) and (b) are obtained by our model on a bimodal network with 50 degree three nodes, 50 degree five nodes, $\gamma = 1$, $\alpha = 0.02$, and $\omega = 0.05$. The results in (c) and (d) are obtained by our model on a Barabási-Albert network with $N = 100$, $\langle k\rangle = 19.8$, $\langle k^2\rangle = 704.674$, $\langle k^3\rangle = 50\,108.802$, $\gamma = 1$, $\alpha = 0.05$, and $\omega = 0.1$. Blue lines represent the approximate results of our model and red lines represent the analytical results which are obtained by performing numerical integration of equations for the system.

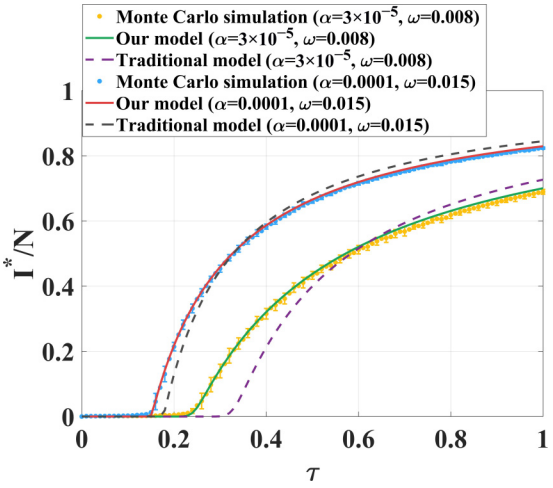

FIG. 5. Epidemic prevalence vs τ for Barabási-Albert networks with random link addition and deletion dynamics under our model. Parameters are $N = 1000$ and $\langle k \rangle = 8$.

behavior under heterogeneous network structures. We further compare the endemic prevalence predicted by our model and the traditional closure model with Monte Carlo simulations, under the same network size, average degree, edge activation rate, and edge termination rate. As shown in Fig. 5, the epidemic threshold predicted by our model is more consistent with Monte Carlo simulations than that predicted by the traditional closure model. Specifically, the epidemic threshold predicted by our model is smaller than that predicted by the traditional closure model. This result can also be analytically derived from Eqs. (8) and (9). We further find that in the whole study regime, the endemic prevalence predicted by our model is more consistent with Monte Carlo simulations than that predicted by the traditional closure model.

V. CONCLUSION

In summary, we have investigated how link temporality affects a prototypical binary-state dynamics, SIS dynamics, on complex networks with arbitrary initial degree distributions. We have analytically obtained the epidemic threshold for SIS dynamics on temporal networks with arbitrary initial degree distributions. For the system close to the epidemic threshold and far away from it, we have derived the approximate result of the endemic equilibrium prevalence with arbitrary degree distributions. Further, we have demonstrated that the system undergoes a continuous transcritical bifurcation from the disease-free state to the endemic state. Our model has been validated to effectively predict the epidemic dynamics. Our study offers a theoretical framework for exploring spreading dynamics on heterogeneous temporal networks and provides valuable insights for epidemic control.

Our work also raises several questions worthy of future pursuit. First, while the model captures essential features of epidemic spreading on dynamic contact networks, it assumes uniform probabilities for the edge activation and termination regardless of the infection status of nodes. However, in real-world scenarios, individuals often adjust their contact behavior based on the health states of both themselves and their contacts. For example, people are more likely to disconnect edges with infected individuals while maintaining connections with healthy ones. To reflect this behavioral heterogeneity, the model can be extended by allowing the edge activation and termination rates to depend explicitly on the infection states of the connected nodes. This state-dependent adaptive mechanism not only provides a more realistic description of individual behavioral responses during epidemic spreading, but may also enhance the predictive capability of the model in heterogeneous network settings, despite the increased analytical complexity it entails. Second, we are able to extend the possibility of predicting critical threshold and analyzing dynamical behavior to the class of binary-state dynamics on temporal complex networks with arbitrary degree distributions. It would be valuable to apply the tractable pair-approximation approach to a wide variety of binary-state dynamics on temporal complex networks with arbitrary degree distributions, such as the voter model [64], Glauber dynamics [65], and the Ising spin model [66]. In addition, it would also be interesting to study if our findings will open a new avenue for understanding how degree distributions affect the dynamical processes other than binary-state dynamics [67,68].

ACKNOWLEDGMENTS

This work is supported by the National Natural Science Foundation of China under Grant No. 62388101 and the National Key Research and Development Program of China under Grant No. 2022YFF0902800.

DATA AVAILABILITY

The data that support the findings of this article are openly available [69].

APPENDIX A: THE STABILITY OF THE DISEASE-FREE STEADY STATE

In this appendix, we prove that the condition $a_3 > 0$ is sufficient to imply that the other two Routh-Hurwitz conditions, $a_1 > 0$ and $a_1 a_2 > a_3$, are also satisfied. We begin by recalling that the Jacobian matrix of Eqs. (3) and (5) at the disease-free equilibrium is

$$\mathrm{DF} = \begin{bmatrix} J_1 & 0 \\ 0 & J_2 \end{bmatrix}, \tag{A1}$$

where

$$J_1 = \begin{bmatrix} -\gamma & \tau & 0 \\ N\alpha & -\alpha - \gamma - \omega + \tau\left(-2 + \frac{k_2}{k_1}\right) & \gamma \\ -\alpha & 2\tau & -\alpha - 2\gamma - \omega \end{bmatrix}$$

and

$$J_2 = \begin{bmatrix} -\alpha - \omega & 0 & 0 \\ 2N\alpha - 3\alpha + \omega & -2\alpha - 2\omega & 0 \\ 3N\alpha - 4\alpha - \omega & 3N\alpha - 6\alpha + 3\omega & -3\alpha - 3\omega \end{bmatrix}.$$

The characteristic polynomial of the matrix J_1 is $\lambda^3 + a_1\lambda^2 + a_2\lambda + a_3$ with $a_1 = 2\alpha + 4\gamma + 2\omega - \tau(\frac{k_2}{k_1} - 2)$, $a_2 = \alpha^2 + 5\alpha\gamma + 2\omega\alpha + 5\gamma^2 + 5\gamma\omega + \omega^2 - \tau(N\alpha - 2\alpha +$

$\frac{k_2}{k_1}\alpha - 4\gamma + 3\gamma\frac{k_2}{k_1} - 2\omega + \frac{k_2}{k_1}\omega)$, and $a_3 = \alpha^2\gamma + 3\alpha\gamma^2 + 2\alpha\gamma\omega + 2\gamma^3 + 3\gamma^2\omega + \gamma\omega^2 - \tau(N\alpha^2 + 2N\alpha\gamma + N\alpha\omega - 3\alpha\gamma + \gamma\alpha\frac{k_2}{k_1} - 2\gamma^2 + 2\gamma^2\frac{k_2}{k_1} - 2\gamma\omega + \gamma\omega\frac{k_2}{k_1})$. According to the Routh-Hurwitz criterion [61], all the roots of the characteristic polynomial have a negative real part, i.e., the steady state is asymptotically stable, once the following three conditions hold:

$$a_1 > 0, \quad a_1 a_2 > a_3, \quad a_3 > 0. \tag{A2}$$

Then we will prove that the condition $a_3 > 0$ implies that both $a_1 > 0$ and $a_1 a_2 > a_3$. To do it, we rewrite the above three coefficients as

$$\begin{aligned} a_1 &= a_{11} - \tau a_{12} = 2\alpha + 4\gamma + 2\omega - \tau\left(\frac{k_2}{k_1} - 2\right), \\ a_2 &= (\alpha + 2\gamma + \omega)(a_{21} - \tau a_{22}), \\ a_3 &= \gamma(\alpha + \gamma + \omega)(a_{31} - \tau a_{32}), \end{aligned} \tag{A3}$$

where $a_{11} = 2\alpha + 4\gamma + 2\omega$, $a_{12} = k_2/k_1 - 2$, $a_{21} = \alpha + 2\gamma + \omega + \gamma(\alpha + \gamma + \omega)/(\alpha + 2\gamma + \omega)$, $a_{22} = k_2/k_1 - 2 + (k_2\gamma)/[k_1(\alpha + 2\gamma + \omega)] + N\alpha/(\alpha + 2\gamma + \omega)$, $a_{31} = \alpha + 2\gamma + \omega$, and $a_{32} = k_2/k_1 - 2 + k_2\gamma/[k_1(\alpha + \gamma + \omega)] + k_1(\alpha + \omega)/(\alpha + \gamma + \omega) + N\alpha/\gamma$. Since we have $a_{11} > a_{21} > a_{31}$ and $a_{12} < a_{22} < a_{32}$, we can easily obtain $a_{11} - \tau a_{12} > a_{21} - \tau a_{22} > a_{31} - \tau a_{32}$. This means $a_3 = \gamma(\alpha + \gamma + \omega)(a_{31} - \tau a_{32}) > 0$ implies $a_1 = a_{11} - \tau a_{12} > a_{31} - \tau a_{32} > 0$. Therefore, $a_3 > 0$ implies $a_1 > 0$.

Further, since $a_{11} - \tau a_{12} = a_{11} - a_{31} + a_{31} - \tau a_{12} > \gamma$, we have

$$\begin{aligned} a_1 a_2 &= a_1(\alpha + 2\gamma + \omega)(a_{21} - \tau a_{22}) \\ &= (a_{11} - \tau a_{12})(\alpha + 2\gamma + \omega)(a_{21} - \tau a_{22}) \\ &> \gamma(\alpha + \gamma + \omega)(a_{31} - \tau a_{32}) = a_3. \end{aligned} \tag{A4}$$

This suggests $a_3 > 0$ implies $a_1 a_2 > a_3$. In summary, our proof demonstrates that once $a_3 > 0$ holds, we have both $a_1 > 0$ and $a_1 a_2 > a_3$.

APPENDIX B: THE CONTINUITY OF TRANSCRITICAL BIFURCATION AT THE DISEASE-FREE EQUILIBRIUM

Here we apply the theorem proposed by Castillo-Chavez and Song to investigate whether the transcritical bifurcation is forward or backward [62]. We simplify the system (1) by applying the conservation equations for the nodes and the edges, and we obtain

$$\begin{aligned} [\dot{I}] &= \tau[SI] - \gamma[I], \\ [\dot{SS}] &= 2\gamma[SI] - 2\tau[SS]\left(\frac{(N - [I])\tilde{A}[SI]}{([SS] + [SI])^2} + \frac{\tilde{B}[SI]}{[SS] + [SI]}\right) \\ &\quad + \alpha[(N - [I])(N - [I] - 1)] - (\alpha + \omega)[SS], \\ [\dot{SI}] &= -(\tau + \gamma)[SI] + \gamma(\langle k\rangle N - [SS] - 2[SI]) \\ &\quad + \tau([SS] - [SI])\left(\frac{(N - [I])\tilde{A}[SI]}{([SS] + [SI])^2} + \frac{\tilde{B}[SI]}{[SS] + [SI]}\right) \\ &\quad + \alpha[(N - [I])[I]] - (\alpha + \omega)[SI]. \end{aligned} \tag{B1}$$

Then we obtain the Jacobian matrix of the system at the disease-free equilibrium, $(0, 0, k_1 N)$, with $\tau = \tau_c$,

$$J(0, 0, k_1 N) = \begin{bmatrix} -\gamma & \tau & 0 \\ N\alpha & \begin{matrix} -\alpha - 3\gamma - \omega \\ +\tau_c(-2 + k_2/k_1) \end{matrix} & -\gamma \\ \alpha(1 - 2N) & 2\gamma - 2\tau_c\left(-1 + \frac{k_2}{k_1}\right) & -\alpha - \omega \end{bmatrix}. \tag{B2}$$

It is obvious that zero is a simple eigenvalue of $J(0, 0, k_1 N)$. The right non-negative eigenvector associated to the zero eigenvalue is

$$m = \begin{bmatrix} R_0 \\ R_1 \\ R_2 \end{bmatrix}, \tag{B3}$$

where $R_0 = \alpha^2 k_1 + 3\alpha\gamma k_1 + 2\alpha k_1\omega + 2\gamma^2 k_1 + 3\gamma k_1\omega + k_1\omega^2$, $R_1 = N\alpha^2 k_1 + 2N\alpha\gamma k_1 + N\alpha k_1\omega - 3\alpha\gamma k_1 + \alpha\gamma k_2 - 2\gamma^2 k_1 + 2\gamma^2 k_2 - 2\gamma k_1\omega + \gamma k_2\omega$, and $R_2 = -2N\alpha^2 k_1 - 4N\alpha\gamma k_1 - 2N\alpha k_1\omega + \alpha^2 k_1 + 5\alpha\gamma k_1 - 2\alpha\gamma k_2 + \alpha k_1\omega + 2\gamma^2 k_1 - 4\gamma^2 k_2 + 2\gamma k_1\omega - 2\gamma k_2\omega$, while the left eigenvector is

$$u = \begin{bmatrix} \frac{N\alpha^2 + 2N\alpha\gamma + N\alpha\omega - \alpha\gamma}{\gamma^2} \\ \frac{\alpha + \omega}{\gamma} \\ -1 \end{bmatrix}. \tag{B4}$$

Therefore, we have

$$\begin{aligned} u^\top m &= 2N\alpha^2 k_1 + 4N\alpha\gamma k_1 + 2N\alpha k_1\omega - \alpha^2 k_1 - 5\alpha\gamma k_1 \\ &\quad + 2\alpha\gamma k_2 - \alpha k_1\omega - 2\gamma^2 k_1 + 4\gamma^2 k_2 - 2\gamma k_1\omega \\ &\quad + 2\gamma k_2\omega + \left(\frac{\alpha + \omega}{\gamma}\right)(N\alpha^2 k_1 + 2N\alpha\gamma k_1 + N\alpha k_1\omega \\ &\quad - 3\alpha\gamma k_1 + \alpha\gamma k_2 - 2\gamma^2 k_1 + 2\gamma^2 k_2 - 2\gamma k_1\omega \\ &\quad + \gamma k_2\omega) + \left(\frac{N\alpha^2 + 2N\alpha\gamma + N\alpha\omega - \alpha\gamma}{\gamma^2}\right)(\alpha^2 k_1 \\ &\quad + 3\alpha\gamma k_1 + 2\alpha k_1\omega + 2\gamma^2 k_1 + 3\gamma k_1\omega + k_1\omega^2), \end{aligned} \tag{B5}$$

where $u^\top$ is the transpose of the left eigenvector u. We normalize the left eigenvector by defining $\tilde{u} = \frac{u}{u^\top m}$, so that the normalization condition $\tilde{u}^\top m = 1$ holds.

By simple algebraic manipulation, we obtain

$$a = \sum_{k,i,j=1}^{3} \tilde{u}_k m_i m_j \frac{\partial^2 F_k}{\partial X_i \partial X_j}(\mathbf{X}, \phi)\big|_{(\mathbf{X}^*, 0)} = \frac{P}{N k_1 u^\top m}, \tag{B6}$$

where $X_1 = [I]$, $X_2 = [SI]$, $X_3 = [SS]$, $F_k(\mathbf{X}) = [\dot{X}_k]$, $k = 1, 2, 3$, $\phi = \tau - \tau_c$, $\mathbf{X}^* = (0, 0, k_1 N)$, and $P = 2(\alpha + \gamma + \omega)(\alpha + 2\gamma + \omega)^2[-N\alpha k_1^3(\alpha + \gamma + \omega)^2 + 2(k_1 - k_2)(\alpha + \gamma + \omega)^2 + \gamma(-k_1 k_3 + k_2^2)(\alpha + 2\gamma + \omega)]$. Since all terms of the inner product between the left eigenvector u and right eigenvector m are positive, we have $u^\top m > 0$. Since $k_1 - k_2 < 0$ and $k_2^2 < k_1 k_3$, we have $P < 0$. Thus, $a < 0$ holds.

On the other hand,

$$b=\sum_{k,i=1}^{3}\tilde{u}_k m_i \frac{\partial^2 F_k}{\partial X_i \partial \phi}(\mathbf{X}^*,0)=\frac{R_1^2}{\gamma^2 k_1 u^\top m}>0. \tag{B7}$$

Therefore, according to the theorem proposed by Castillo-Chavez and Song, $a<0$ and $b>0$ indicate that the transcritical bifurcation at the epidemic threshold is continuous.

APPENDIX C: THE ANALYTICAL APPROXIMATIONS OF THE ENDEMIC EQUILIBRIUM

Here we apply the regular perturbation method to derive the endemic equilibrium for two cases: the system close to the epidemic threshold ($\delta\approx\delta_c$, i.e., $\tau\approx\tau_c$) and far away from it ($\delta\gg\delta_c$, i.e., $\tau\gg\tau_c$). In order to turn the task of deriving the endemic equilibrium from Eq. (1) into a perturbation problem, when the system reaches the endemic equilibrium, we nondimensionalize the system and reduce the number of independent parameters, which leads to the following equations:

$$\begin{aligned}
0&=\dot{v}=w-k_1\delta x,\\
0&=\dot{w}=k_1\delta x-w,\\
0&=\dot{x}=z-(\delta+1)x+\frac{k_2^2-k_1k_3}{k_2-k_1^2}\frac{\delta}{k_1}\frac{vx(y-x)}{(x+y)^2}\\
&\quad+\left(\frac{k_3-k_1k_2}{k_2-k_1^2}-1\right)\delta\frac{x(y-x)}{x+y}+\tilde{\alpha}vw\frac{N}{k_1}-(\tilde{\alpha}+\tilde{\omega})x,\\
0&=\dot{y}=-\frac{k_2^2-k_1k_3}{k_2-k_1^2}\frac{2\delta}{k_1}\frac{vxy}{(x+y)^2}-2\left(\frac{k_3-k_1k_2}{k_2-k_1^2}-1\right)\frac{\delta xy}{x+y}\\
&\quad+2x+\tilde{\alpha}\frac{v}{k_1}(vN-1)-(\tilde{\alpha}+\tilde{\omega})y,\\
0&=\dot{z}=-2z+2\delta x+\frac{k_2^2-k_1k_3}{k_2-k_1^2}\frac{2\delta}{k_1}\frac{vx^2}{(x+y)^2}-(\tilde{\alpha}+\tilde{\omega})z\\
&\quad+2\left(\frac{k_3-k_1k_2}{k_2-k_1^2}-1\right)\frac{\delta x^2}{x+y}+\tilde{\alpha}\frac{w}{k_1}(wN-1),
\end{aligned} \tag{C1}$$

where $v=[S]/N$, $w=[I]/N$, $x=[SI]/k_1N$, $y=[SS]/k_1N$, $z=[II]/k_1N$, $T=t/\gamma$, $\tilde{\alpha}=\alpha/\gamma$, $\tilde{\omega}=\omega/\gamma$, $\delta=\tau/\gamma$, and $\delta_c=\tau_c/\gamma=\frac{(\alpha+1+\omega)(\alpha+2+\omega)}{(\alpha+1+\omega)[N\alpha+2(k_2/k_1-1)]-\omega}$. Since the conservation equations hold for nodes and edges, i.e., $[S]+[I]=N$ and $[SS]+2[SI]+[II]=\langle k\rangle N$, we have $v+w=1$ and $2x+y+z=1$. After substituting these into Eqs. (C1), we obtain a system of two coupled polynomial equations,

$$\begin{aligned}
M(x,y)&=\left(\frac{\delta_c}{\delta}\right)^2\left[(1-2x-y)-(\tilde{\alpha}+\tilde{\omega})\left(x+\frac{1}{2}y\right)\right.\\
&\quad\left.+\left(\frac{\tilde{\alpha}N}{2k_1}-\frac{\tilde{\alpha}}{2k_1}\right)\right](x+y)^2+\frac{\delta_c}{\delta}\left[-\delta_c x(x+y)^2\right.\\
&\quad\left.-\lambda x^2-\mu x^2(x+y)+\frac{\tilde{\alpha}}{2k_1}\sigma x(x+y)^2\right]\\
&\quad+\lambda\sigma x^3-\frac{N\tilde{\alpha}}{2k_1}\sigma^2x^2(x+y)^2=0,\\
N(x,y)&=\left(\frac{\delta_c}{\delta}\right)^2\left[2x-(\tilde{\alpha}+\tilde{\omega})y+\tilde{\alpha}\frac{N}{k_1}-\frac{\tilde{\alpha}}{k_1}\right](x+y)^2\\
&\quad+\frac{\delta_c}{\delta}\left[-2\lambda xy-2\mu xy(x+y)-2\frac{\tilde{\alpha}N}{k_1}\sigma x(x+y)^2\right.\\
&\quad\left.+\frac{\tilde{\alpha}}{k_1}\sigma x(x+y)^2\right]+2\lambda\sigma x^2y+\frac{N\tilde{\alpha}}{k_1}\sigma^2x^2(x+y)^2\\
&=0,
\end{aligned} \tag{C2}$$

where $\sigma=k_1\delta_c$, $\lambda=(k_2^2-k_1k_3)/(k_2-k_1^2)\delta_c/k_1$, and $\mu=[(k_3-k_1k_2)/(k_2-k_1^2)-1]\delta_c$. Note that we replace δ with $\delta_c\cdot\frac{\delta}{\delta_c}$ to find the small parameter in the system of polynomial equations. We first consider the situation that the system is close to the epidemic threshold, i.e., $\delta\approx\delta_c$ or $\tau\approx\tau_c$. We replace $\frac{\delta_c}{\delta}$ with $1-\eta$ in Eqs. (C2), where η is the dimensionless small parameter, leading to

$$\begin{aligned}
M(x,y)&=(1-\eta)^2(1-2x-y)\left(\frac{\tilde{\alpha}+\tilde{\omega}+2}{2}\right)(x+y)^2\\
&\quad+(1-\eta)\left[-\delta_c x(x+y)^2-\lambda x^2\right.\\
&\quad\left.-\mu x^2(x+y)+\frac{\tilde{\alpha}}{2k_1}\sigma x(x+y)^2\right]\\
&\quad+\lambda\sigma x^3-\frac{N\tilde{\alpha}}{2k_1}\sigma^2x^2(x+y)^2\\
&=0,
\end{aligned} \tag{C3}$$

$$\begin{aligned}
N(x,y)&=(1-\eta)^2(2x-(\tilde{\alpha}+\tilde{\omega})(y-1))(x+y)^2\\
&\quad+(1-\eta)\left[-2\lambda xy-2\mu xy(x+y)\right.\\
&\quad\left.-2(\tilde{\alpha}+\tilde{\omega})\sigma x(x+y)^2-\frac{\tilde{\alpha}}{k_1}\sigma x(x+y)^2\right]\\
&\quad+2\lambda\sigma x^2y+\frac{N\tilde{\alpha}}{k_1}\sigma^2x^2(x+y)^2=0.
\end{aligned} \tag{C4}$$

By applying the implicit function theorem to linearize Eq. (C3) around the point $(x,y)=(0,1)$, we obtain

$$\begin{aligned}
y&=\tilde{y}-\frac{M_x(\tilde{x},\tilde{y})}{M_y(\tilde{x},\tilde{y})}(x-\tilde{x})\\
&=1-\left(2+\frac{C}{1-\eta}\right)x,
\end{aligned} \tag{C5}$$

where $M_x(x,y)$ and $M_y(x,y)$ denote the partial derivatives of $M(x,y)$ with respect to x and y, respectively, $(\tilde{x},\tilde{y})=(0,1)$ and $C=\frac{(2-\tilde{\alpha})\delta_c}{\tilde{\alpha}+\tilde{\omega}+2}$. Then we substitute Eq. (C5) into the first term of $N(x,y)$ in Eq. (C4), and divide the resulting formula of $N(x,y)$ by x, which yields

$$\begin{aligned}
0=N(x,y)/x&=(1-\eta)^2\left[2+(\tilde{\alpha}+\tilde{\omega})\left(2+\frac{C}{1-\eta}\right)\right](x+y)^2\\
&\quad+(1-\eta)\left[-2\lambda y-2\mu y(x+y)-2(\tilde{\alpha}+\tilde{\omega})\right.\\
&\quad\left.\cdot\sigma(x+y)^2-\frac{\tilde{\alpha}\sigma}{k_1}(x+y)^2\right]+2\lambda\sigma xy\\
&\quad+\frac{N\tilde{\alpha}}{k_1}\sigma^2x(x+y)^2.
\end{aligned} \tag{C6}$$

Further, we perform asymptotic expansions in terms of η for the variables x, y, and $\frac{1}{1-\eta}$ around x_0, y_0, and 0, respectively, which are

$$x = x_0 + x_1\eta + x_2\eta^2 + x_3\eta^3 + \cdots, \tag{C7}$$

$$\begin{aligned} y &= y_0 + y_1\eta + y_2\eta^2 + y_3\eta^3 + \cdots \\ &= 1 - (2+C)x_0 - (Cx_0 + (2+C)x_1)\eta - [Cx_0 + Cx_1 + (2+C)x_2]\eta^2 + \cdots, \end{aligned} \tag{C8}$$

$$\frac{1}{(1-\eta)} = 1 + \eta + \eta^2 + \eta^3 + \cdots. \tag{C9}$$

After substituting Eqs. (C7)–(C9) into Eq. (C6) and collecting terms of equal powers of η, the right-hand side of Eq. (C6) becomes a polynomial in η, while the left-hand side is zero. Therefore, the coefficients of each order of η are zero.

Since the $O(1)$ term in η is zero, we have

$$\begin{aligned} &C\tilde{\alpha} + C\tilde{\omega} - \frac{2N\tilde{\alpha}\sigma}{k_1} + 2\tilde{\alpha} + \frac{\tilde{\alpha}\sigma}{k_1} - 2\lambda - 2\mu + 2\tilde{\omega} + 2 + x_0\Bigg(-2C^2\tilde{\alpha} - 2C^2\tilde{\omega} + \frac{4CN\tilde{\alpha}\sigma}{k_1} - 6C\tilde{\alpha} - \frac{2C\tilde{\alpha}\sigma}{k_1} + 2C\lambda \\ &+ 4C\mu - 6C\tilde{\omega} - 4C + \frac{N\tilde{\alpha}\sigma^2}{k_1} + \frac{4N\tilde{\alpha}\sigma}{k_1} - 4\tilde{\alpha} - \frac{2\tilde{\alpha}\sigma}{k_1} + 2\lambda\sigma + 4\lambda + 6\mu - 4\tilde{\omega} - 4\Bigg) + x_0^2\Bigg(C^3\tilde{\alpha} + C^3\tilde{\omega} - \frac{2C^2N\tilde{\alpha}\sigma}{k_1} \\ &+ 4C^2\tilde{\alpha} + \frac{C^2\sigma}{k_1} - 2C^2\mu + 4C^2\tilde{\omega} + 2C^2 - \frac{2CN\tilde{\alpha}\sigma^2}{k_1} - \frac{4CN\tilde{\alpha}\sigma}{k_1} + 5C\tilde{\alpha} + \frac{2C\tilde{\alpha}\sigma}{k_1} - 2C\lambda\sigma - 6C\mu + 5C\tilde{\omega} + 4C \\ &- \frac{2N\tilde{\alpha}\sigma^2}{k_1} - \frac{2N\tilde{\alpha}\sigma}{k_1} + 2\tilde{\alpha} + \frac{\tilde{\alpha}\sigma}{k_1} - 4\lambda\sigma - 4\mu + 2\tilde{\omega} + 2\Bigg) + x_0^3\Bigg(\frac{C^2N\tilde{\alpha}\sigma^2}{k_1} + \frac{2CN\tilde{\alpha}\sigma^2}{k_1} + \frac{N\tilde{\alpha}\sigma^2}{k_1}\Bigg) = 0. \end{aligned} \tag{C10}$$

Since we have $k_1 = \tilde{\alpha}(N-1)/(\tilde{\alpha}+\tilde{\omega})$ and $C = (2-\tilde{\alpha})\delta_c/(\tilde{\alpha}+\tilde{\omega}+2)$, the constant term of Eq. (C10) is zero. Thus, we have $x_0 = 0$ and $y_0 = 1 - (2+C)x_0 = 1$.

Next, due to the coefficient of the $O(\eta)$ term being zero, we have

$$\begin{aligned} &-C\tilde{\alpha} - C\tilde{\omega} + \frac{2N\tilde{\alpha}\sigma}{k_1} - 4\tilde{\alpha} - \frac{\tilde{\alpha}\sigma}{k_1} + 2\lambda + 2\mu - 4\tilde{\omega} - 4 + x_1\Bigg(-2C^2\tilde{\alpha} - 2C^2\tilde{\omega} + \frac{4CN\tilde{\alpha}\sigma}{k_1} - 6C\tilde{\alpha} - \frac{2C\tilde{\alpha}\sigma}{k_1} \\ &+ 2C\lambda + 4C\mu - 6C\tilde{\omega} - 4C + \frac{N\tilde{\alpha}\sigma^2}{k_1} + \frac{4N\tilde{\alpha}\sigma}{k_1} - 4\tilde{\alpha} - \frac{2\tilde{\alpha}\sigma}{k_1} + 2\lambda + 4\lambda + 6\mu - 4\tilde{\omega} - 4\Bigg) = 0. \end{aligned} \tag{C11}$$

After substituting $k_1 = \frac{\tilde{\alpha}(N-1)}{\tilde{\alpha}+\tilde{\omega}}$ and $C = \frac{(2-\tilde{\alpha})\delta_c}{\tilde{\alpha}+\tilde{\omega}+2}$ into Eq. (C11), we obtain

$$x_1 = \frac{2(\tilde{\alpha}+\tilde{\omega}+1)}{-2\lambda C + N\tilde{\alpha}k_1\delta_c^2 + 2\lambda\sigma + 2\mu}. \tag{C12}$$

Further, by retaining the first-order term and second-order terms of the asymptotic expansion x in Eq. (C7) and neglecting the high-order terms, we derive the approximate endemic equilibrium for the system close to the epidemic threshold as

$$\begin{aligned} x_1^* &= \frac{2k_1\gamma^2(\alpha+\gamma+\omega)(\alpha+2\gamma+\omega)\left(k_2-k_1^2\right)}{k_1\tau_c\left[N\alpha k_1\tau_c\left(k_2-k_1^2\right)+2\gamma\tau_c\left(k_2^2-k_1k_3\right)\right.}\eta \\ &\quad \left.+2\gamma^2\left(k_3-k_2k_1-k_2+k_1^2\right)\right](\alpha+2\gamma+\omega) \\ &\quad -2\tau_c^2\gamma(2\gamma-\alpha)\left(k_2^2-k_1k_3\right), \\ w_1^* &= \frac{2k_1^2\gamma\tau_c(\alpha+\gamma+\omega)(\alpha+2\gamma+\omega)}{k_1\tau_c\left[N\alpha k_1\tau_c\left(k_2-k_1^2\right)+2\gamma\tau_c\left(k_2^2-k_1k_3\right)\right.}\eta \\ &\quad \left.+2\gamma^2\left(k_3-k_2k_1-k_2+k_1^2\right)\right](\alpha+2\gamma+\omega) \\ &\quad -2\tau_c^2\gamma(2\gamma-\alpha)\left(k_2^2-k_1k_3\right). \end{aligned} \tag{C13}$$

Then we consider another situation that the system is far away from the epidemic threshold, i.e., $\delta \gg \delta_c$ or $\tau \gg \tau_c$. We replace $\frac{\delta_c}{\delta}$ in Eqs. (C2) with the small nondimensional parameter $\varepsilon = \frac{\delta_c}{\delta}$ and derive the following equations by performing some straightforward algebraic computations:

$$\begin{aligned} 0 = Q(x,y) &= \varepsilon^2(x+y)^2\{[2x-(\tilde{\alpha}+\tilde{\omega})(y-1)] \\ &\quad +(1-2x-y)(\tilde{\alpha}+\tilde{\omega}+2)\} \\ &\quad +\varepsilon[-2\delta_c x(x+y)^2 - 2\lambda x^2 - 2\lambda xy \\ &\quad -2\mu x^2(x+y) - 2\mu xy(x+y) \\ &\quad -2(\tilde{\alpha}+\tilde{\omega})\sigma x(x+y)^2] + 2\lambda\sigma x^2y + 2\lambda\sigma x^3, \end{aligned} \tag{C14}$$

$$\begin{aligned} 0 = T(x,y) &= \varepsilon^2[2x-(\tilde{\alpha}+\tilde{\omega})(y-1)](x+y)^2 \\ &\quad +\varepsilon\Bigg[-2\lambda xy - 2\mu xy(x+y) \\ &\quad -2\sigma x(\tilde{\alpha}+\tilde{\omega})(x+y)^2 - \frac{\tilde{\alpha}}{k_1}\sigma x(x+y)^2\Bigg] \\ &\quad +2\lambda\sigma x^2y + \frac{N\tilde{\alpha}}{k_1}\sigma^2x^2(x+y)^2. \end{aligned} \tag{C15}$$

Since the recovery rate is much smaller than the transmission rate for $\delta \gg \delta_c$, the disease is expected to spread almost the entire network with only a small number of remaining $[SS]$ edges, which implies $y \approx 0$. In this case, the endemic equilibrium can be viewed as a perturbation to the steady state, $(x, y) = (\Phi, 0)$. By solving $Q(\Phi, 0) = 0$ for Φ, we obtain

$$\Phi = \frac{\varepsilon(\tilde{\alpha}\varepsilon - \lambda + \tilde{\omega}\varepsilon + \varepsilon)}{\tilde{\alpha}\sigma\varepsilon + \tilde{\alpha}\varepsilon^2 + \delta_c\varepsilon - \lambda\sigma + \mu\varepsilon + \tilde{\omega}\sigma\varepsilon + \tilde{\omega}\varepsilon^2 + \varepsilon^2}. \tag{C16}$$

By applying the implicit function theorem to linearize Eq. (C14) around the point $(x, y) = (\Phi, 0)$, we obtain

$$y = -\frac{Q_x}{Q_y}\bigg|_{(\Phi,0)} (x - \Phi) = \psi(x - \Phi), \tag{C17}$$

where Q_x and Q_y denote the partial derivatives of $Q(x, y)$ with respect to x and y, respectively, $\psi = (\tilde{\alpha}\varepsilon - \lambda + \tilde{\omega}\varepsilon + \varepsilon)(\tilde{\alpha}\sigma\varepsilon + \tilde{\alpha}\varepsilon^2 + \delta_c\varepsilon - \lambda\sigma + \mu\varepsilon + \tilde{\omega}\sigma\varepsilon + \tilde{\omega}\varepsilon^2 + \varepsilon^2)/\{\varepsilon[-(\tilde{\alpha} + \tilde{\omega} + 1)^2\varepsilon^2 + 2\lambda\varepsilon(\tilde{\alpha} + \tilde{\omega} + 1) + \lambda(\delta_c + \mu - \sigma)]\}$.

Then we perform asymptotic expansions in terms of ε for the variables Φ, ψ, x, and y around Φ_0, ψ_{-1}, x_0, and y_0, respectively, leading to

$$\begin{aligned}\Phi(\varepsilon) &= \Phi_0 + \Phi_1\varepsilon + \Phi_2\varepsilon^2 + O(\varepsilon^3)\\ &= 0 + \frac{1}{\sigma}\varepsilon + \frac{\delta_c + \mu - \sigma}{\lambda\sigma^2}\varepsilon^2 + O(\varepsilon^3),\end{aligned} \tag{C18}$$

$$\begin{aligned}\psi(\varepsilon) &= \psi_{-1}\frac{1}{\varepsilon} + \psi_0 + O(\varepsilon)\\ &= \frac{\lambda\sigma}{\delta_c + \mu - \sigma}\frac{1}{\varepsilon} - 2\lambda\sigma(\tilde{\alpha} + \tilde{\omega} + 1)\\ &\quad + (\delta_c + \mu - \sigma)[-\tilde{\alpha}\sigma - \delta_c - \mu\\ &\quad + \frac{-\tilde{\omega}\sigma - \sigma(\tilde{\alpha} + \tilde{\omega} + 1)]}{(\delta_c + \mu - \sigma)^2} + O(\varepsilon),\end{aligned} \tag{C19}$$

$$x = x_0 + x_1\varepsilon + x_2\varepsilon^2 + x_3\varepsilon^3 + \cdots, \tag{C20}$$

$$y = y_{-1}\varepsilon^{-1} + y_0 + y_1\varepsilon + y_2\varepsilon^2 + y_3\varepsilon^3 + \cdots. \tag{C21}$$

Substituting Eqs. (C18)–(C20) into Eq. (C17), we have

$$\begin{aligned}y &= \psi(x - \Phi)\\ &= \psi_{-1}x_0\varepsilon^{-1} + (\psi_{-1}x_1 + \psi_0x_0 - \psi_{-1}\Phi_1)\\ &\quad + (\psi_{-1}x_2 + \psi_0x_1 - \psi_{-1}\Phi_2 - \psi_0\Phi_1)\varepsilon + O(\varepsilon^2).\end{aligned} \tag{C22}$$

By substituting Eqs. (C20) and (C21) into Eq. (C15) and collecting terms of equal powers of ε, we obtain that the right-hand side of Eq. (C15) is a polynomial in ε, while the left-hand side is zero. Therefore, we obtain that the coefficients of each order of ε are zero.

Since the $O(1)$ term in ε is zero, we have

$$x_0 = y_{-1} = 0, \tag{C23}$$

which suggests the coefficients of the $O(\varepsilon)$, $O(\varepsilon^2)$, and $O(\varepsilon^3)$ terms are all zero. Further, since the coefficient of the $O(\varepsilon^4)$ term is zero, we obtain $y_0 = 0$. Based on the formula $y_0 = (\psi_{-1}x_1 + \psi_0x_0 - \psi_{-1}\Phi_1) = \psi_{-1}(x_1 - \Phi_1)$ in Eq. (C22), we obtain

$$x_1 = \Phi_1 = \frac{1}{\sigma}, \tag{C24}$$

which suggests that the coefficient of the $O(\varepsilon^5)$ term is zero. Due to the coefficient of the $O(\varepsilon^6)$ term being zero, we obtain $y_1 = 0$. Based on the formula $y_1 = \psi_{-1}(x_2 - \Phi_2) + \psi_0(x_1 - \Phi_1) = \psi_{-1}(x_2 - \Phi_2)$ in Eq. (C22), we obtain

$$x_2 = \Phi_2 = \frac{\delta_c + \mu - \sigma}{\lambda\sigma^2}. \tag{C25}$$

By applying (C23)–(C25), and retaining only the first-order term and second-order term of the asymptotic expansion of x in Eq. (C20), we obtain the approximate endemic equilibrium when the system is far away from the epidemic threshold as

$$\begin{aligned}x_2^* &= \frac{\gamma}{k_1\tau_c}\varepsilon - \frac{\left(k_1^3 + k_3 - 2k_1k_2\right)\gamma^2}{\left(k_1k_3 - k_2^2\right)k_1\tau_c^2}\varepsilon^2,\\ w_2^* &= 1 - \frac{\left(k_1^3 + k_3 - 2k_1k_2\right)\gamma}{\left(k_1k_3 - k_2^2\right)\tau_c}\varepsilon.\end{aligned} \tag{C26}$$

[1] A. Barrat, M. Barthélemy, and A. Vespignani, *Dynamical Processes on Complex Networks* (Cambridge University Press, Cambridge, 2008).

[2] M. Newman, *Networks* (Oxford University Press, Oxford, 2018).

[3] C. Castellano, S. Fortunato, and V. Loreto, Statistical physics of social dynamics, Rev. Mod. Phys. **81**, 591 (2009).

[4] D. Li, W. Xie, D. Han, and M. Sun, A multi-information epidemic spreading model on a two-layer network, Inf. Sci. **651**, 119723 (2023).

[5] W. Wang, Y. Nie, W. Li, T. Lin, M.-S. Shang, S. Su, Y. Tang, Y.-C. Zhang, and G.-Q. Sun, Epidemic spreading on higher-order networks, Phys. Rep. **1056**, 1 (2024).

[6] Y. Wang, L. Tu, X. Wang, and Y. Guo, Evolutionary vaccination game considering intra-seasonal strategy shifts regarding multi-seasonal epidemic spreading, Chaos Solitons Fract. **180**, 114419 (2024).

[7] J. Zhang, C. Yang, Z. Jin, and J. Li, Dynamics analysis of SIR epidemic model with correlation coefficients and clustering coefficient in networks, J. Theor. Biol. **449**, 1 (2018).

[8] R. C. Barnard, L. Berthouze, P. L. Simon, and I. Z. Kiss, Epidemic threshold in pairwise models for clustered networks: Closures and fast correlations, J. Math. Biol. **79**, 823 (2019).

[9] Q. Yin, Z. Wang, C. Xia, and C. T. Bauch, Impact of co-evolution of negative vaccine-related information, vaccination behavior and epidemic spreading in multilayer networks, Commun. Nonlinear Sci. Numer. Simul. **109**, 106312 (2022).

[10] J.-X. Yang, Z.-P. Cao, and Y. Lu, Contagion dynamics on a compound model, Appl. Math. Comput. **460**, 128293 (2024).

[11] P. Holme and J. Saramäki, Temporal networks, Phys. Rep. **519**, 97 (2012).

[12] N. Masuda, K. Klemm, and V. M. Eguíluz, Temporal networks: Slowing down diffusion by long lasting interactions, Phys. Rev. Lett. **111**, 188701 (2013).

[13] J.-C. Delvenne, R. Lambiotte, and L. E. Rocha, Diffusion on networked systems is a question of time or structure, Nat. Commun. **6**, 7366 (2015).
[14] I. Scholtes, N. Wider, R. Pfitzner, A. Garas, C. J. Tessone, and F. Schweitzer, Causality-driven slow-down and speed-up of diffusion in non-Markovian temporal networks, Nat. Commun. **5**, 5024 (2014).
[15] T. Hiraoka and H.-H. Jo, Correlated bursts in temporal networks slow down spreading, Sci. Rep. **8**, 15321 (2018).
[16] P. Van Mieghem and R. van de Bovenkamp, Non-Markovian infection spread dramatically alters the susceptible-infected-susceptible epidemic threshold in networks, Phys. Rev. Lett. **110**, 108701 (2013).
[17] S. Cure, F. G. Pflug, and S. Pigolotti, Exponential rate of epidemic spreading on complex networks, Phys. Rev. E **111**, 044311 (2025).
[18] A. Li, L. Zhou, Q. Su, S. P. Cornelius, Y.-Y. Liu, L. Wang, and S. A. Levin, Evolution of cooperation on temporal networks, Nat. Commun. **11**, 2259 (2020).
[19] Y. Meng, A. McAvoy, and A. Li, Promoting collective cooperation through temporal interactions, Proc. Natl. Acad. Sci. USA **122**, e2509575122 (2025).
[20] S. Nag Chowdhury, S. Kundu, M. Duh, M. Perc, and D. Ghosh, Cooperation on interdependent networks by means of migration and stochastic imitation, Entropy **22**, 485 (2020).
[21] M. S. Anwar, S. Rakshit, D. Ghosh, and E. M. Bollt, Stability analysis of intralayer synchronization in time-varying multilayer networks with generic coupling functions, Phys. Rev. E **105**, 024303 (2022).
[22] S. Rakshit, S. Majhi, and D. Ghosh, Stability analysis of synchronization in long-range temporal networks using theory of dichotomy, Chaos **34**, 033114 (2024).
[23] S. N. Chowdhury and H. Meyer-Ortmanns, Metastability induced by non-reciprocal adaptive couplings in Kuramoto models, Front. Netw. Physiol. **6**, 1774273 (2026).
[24] S. N. Chowdhury, S. Majhi, M. Ozer, D. Ghosh, and M. Perc, Synchronization to extreme events in moving agents, New J. Phys. **21**, 073048 (2019).
[25] S. N. Chowdhury, S. Majhi, and D. Ghosh, Distance dependent competitive interactions in a frustrated network of mobile agents, IEEE Trans. Network Sci. Eng. **7**, 3159 (2020).
[26] T. Onaga, J. P. Gleeson, and N. Masuda, Concurrency-induced transitions in epidemic dynamics on temporal networks, Phys. Rev. Lett. **119**, 108301 (2017).
[27] Y. Long, X. Liu, and Z. Liu, Temporal stability of the dynamic resting-state functional brain network: Current measures, clinical research progress, and future perspectives, Brain Sci. **13**, 429 (2023).
[28] G. Miritello, E. Moro, and R. Lara, Dynamical strength of social ties in information spreading, Phys. Rev. E **83**, 045102(R) (2011).
[29] M. Karsai, M. Kivelä, R. K. Pan, K. Kaski, J. Kertész, A.-L. Barabási, and J. Saramäki, Small but slow world: How network topology and burstiness slow down spreading, Phys. Rev. E **83**, 025102(R) (2011).
[30] L. Ferreri, P. Bajardi, M. Giacobini, S. Perazzo, and E. Venturino, Interplay of network dynamics and heterogeneity of ties on spreading dynamics, Phys. Rev. E **90**, 012812 (2014).
[31] N. Perra, B. Gonçalves, R. Pastor-Satorras, and A. Vespignani, Activity driven modeling of time varying networks, Sci. Rep. **2**, 469 (2012).
[32] E. Valdano, L. Ferreri, C. Poletto, and V. Colizza, Analytical computation of the epidemic threshold on temporal networks, Phys. Rev. X **5**, 021005 (2015).
[33] C.-R. Cai, Y.-Y. Nie, and P. Holme, Epidemic criticality in temporal networks, Phys. Rev. Res. **6**, L022017 (2024).
[34] Z. Luo, S. Li, Z. Jiang, and W. Chen, Social contagion models on adaptive simplicial complexes, Physica A **679**, 131010 (2025).
[35] G. V. Clemente and D. Garlaschelli, Linking through time: Memory-enhanced community discovery in temporal networks, Phys. Rev. Res. **6**, 043204 (2024).
[36] B. Chen, G. Hou, and A. Li, Temporal local clustering coefficient uncovers the hidden pattern in temporal networks, Phys. Rev. E **109**, 064302 (2024).
[37] L. Zino and M. Cao, Analysis, prediction, and control of epidemics: A survey from scalar to dynamic network models, IEEE Circuits Syst. Mag. **21**, 4 (2021).
[38] T. Shiraga and S. Kijima, An analysis of load-balancing algorithms on edge-Markovian evolving graphs, J. Comput. Syst. Sci. **160**, 103797 (2026).
[39] M. Ogura and V. M. Preciado, Stability of spreading processes over time-varying large-scale networks, IEEE Trans. Network Sci. Eng. **3**, 44 (2016).
[40] E. Volz and L. A. Meyers, Susceptible–infected–recovered epidemics in dynamic contact networks, Proc. R. Soc. B **274**, 2925 (2007).
[41] E. Volz and L. A. Meyers, Epidemic thresholds in dynamic contact networks, J. R. Soc. Interface **6**, 233 (2009).
[42] A. Szabó, P. L. Simon, and I. Z. Kiss, Detailed study of bifurcations in an epidemic model on a dynamic network, Differ. Equ. Appl. **4**, 277 (2012).
[43] M. Taylor, T. J. Taylor, and I. Z. Kiss, Epidemic threshold and control in a dynamic network, Phys. Rev. E **85**, 016103 (2012).
[44] A. Szabó-Solticzky, L. Berthouze, I. Z. Kiss, and P. L. Simon, Oscillating epidemics in a dynamic network model: Stochastic and mean-field analysis, J. Math. Biol. **72**, 1153 (2016).
[45] C. Corcoran and J. M. Clark, Adaptive network modeling of social distancing interventions, J. Theor. Biol. **546**, 111151 (2022).
[46] I. Tunc, M. S. Shkarayev, and L. B. Shaw, Epidemics in adaptive social networks with temporary link deactivation, J. Stat. Phys. **151**, 355 (2013).
[47] M. S. Shkarayev, I. Tunc, and L. B. Shaw, Epidemics with temporary link deactivation in scale-free networks, J. Phys. A: Math. Theor. **47**, 455006 (2014).
[48] T. Gross, C. J. Dommar D'Lima, and B. Blasius, Epidemic dynamics on an adaptive network, Phys. Rev. Lett. **96**, 208701 (2006).
[49] F. L. Pinheiro, F. C. Santos, and J. M. Pacheco, Linking individual and collective behavior in adaptive social networks, Phys. Rev. Lett. **116**, 128702 (2016).
[50] S. V. Scarpino, A. Allard, and L. Hébert-Dufresne, The effect of a prudent adaptive behaviour on disease transmission, Nat. Phys. **12**, 1042 (2016).

[51] P. G. Sun, W. Che, Y. Quan, S. Wang, and Q. Miao, Random networks are heterogeneous exhibiting a multi-scaling law, Physica A **587**, 126479 (2022).

[52] E. Ubaldi, N. Perra, M. Karsai, A. Vezzani, R. Burioni, and A. Vespignani, Asymptotic theory of time-varying social networks with heterogeneous activity and tie allocation, Sci. Rep. **6**, 35724 (2016).

[53] N. Gozzi, M. Scudeler, D. Paolotti, A. Baronchelli, and N. Perra, Self-initiated behavioral change and disease resurgence on activity-driven networks, Phys. Rev. E **104**, 014307 (2021).

[54] E. Valdano, M. R. Fiorentin, C. Poletto, and V. Colizza, Epidemic threshold in continuous-time evolving networks, Phys. Rev. Lett. **120**, 068302 (2018).

[55] G. V. Clemente, C. J. Tessone, and D. Garlaschelli, Temporal networks with node-specific memory: Unbiased inference of transition probabilities, relaxation times, and structural breaks, Phys. Rev. Res. **6**, 043257 (2024).

[56] M. J. Keeling, D. A. Rand, and A. J. Morris, Correlation models for childhood epidemics, Proc. R. Soc. Lond. B **264**, 1149 (1997).

[57] M. J. Keeling and K. T. D. Eames, Networks and epidemic models, J. R. Soc. Interface **2**, 295 (2005).

[58] P. L. Simon and I. Z. Kiss, Super compact pairwise model for SIS epidemic on heterogeneous networks, J. Complex Netw. **4**, 187 (2016).

[59] T. House and M. J. Keeling, Insights from unifying modern approximations to infections on networks, J. R. Soc. Interface **8**, 67 (2011).

[60] I. Z. Kiss, L. Berthouze, T. J. Taylor, and P. L. Simon, Modelling approaches for simple dynamic networks and applications to disease transmission models, Proc. R. Soc. A **468**, 1332 (2012).

[61] M. Rao and P. Rao, Some more comments on "on the Routh-Hurwitz criterion", IEEE Trans. Autom. Control **20**, 714 (1975).

[62] C. Castillo-Chavez and B. Song, Dynamical models of tuberculosis and their applications, Math. Biosci. Eng. **1**, 361 (2004).

[63] C. Corcoran and A. Hastings, A low-dimensional network model for an SIS epidemic: Analysis of the super compact pairwise model, Bull. Math. Biol. **83**, 77 (2020).

[64] V. Sood and S. Redner, Voter model on heterogeneous graphs, Phys. Rev. Lett. **94**, 178701 (2005).

[65] C. Castellano and R. Pastor-Satorras, Zero temperature Glauber dynamics on complex networks, J. Stat. Mech. (2006) P05001.

[66] S. N. Dorogovtsev, A. V. Goltsev, and J. F. F. Mendes, Ising model on networks with an arbitrary distribution of connections, Phys. Rev. E **66**, 016104 (2002).

[67] J. Li, Z. Jin, and Y. Yuan, Effect of adaptive rewiring delay in a SIS network epidemic model, Math. Biosci. Eng. **16**, 8092 (2019).

[68] I. Tunc and L. B. Shaw, Effects of community structure on epidemic spread in an adaptive network, Phys. Rev. E **90**, 022801 (2014).

[69] Z. Luo, SIS model on temporal networks, https://github.com/ztluo123/epidemic-dynamics-on-temporal-complex-networks.